

Testing a generic GEANT4 detector simulation using $H \rightarrow \gamma\gamma$ events

Olga Sunneborn Gudnadottir

October 12, 2018

Abstract

A generic GEANT4 detector simulation developed at Uppsala University has been tested for accuracy and resolution using $H \rightarrow \gamma\gamma$ events generated in MADGRAPH5_AMC@NLO and PYTHIA8. A sliding window photon reconstruction algorithm was implemented for the tests. A Higgs peak was reconstructed with a mean value of 120.9 GeV and a standard deviation of 1.9 GeV.

Contents

1	Introduction	3
1.1	Detector simulations	3
1.2	The need for a new detector simulation	4
1.3	Project outline	4
2	Background	5
2.1	Detector simulations	5
2.1.1	Detectors	5
2.1.2	Simulations	6
2.1.3	Event generators	7
2.2	ROOT	9
2.2.1	Two important classes	9
2.2.2	Using ROOT	9
2.3	Generic Detector Simulation	9
2.3.1	Using the Generic Detector Simulation	12
2.4	Benchmark process $H \rightarrow \gamma\gamma$	12
3	Photon Reconstruction	14
3.1	Seed positions	14
3.2	Removing duplicates	15
3.3	Cluster filling	15
4	Analysis	16
5	Results	17
6	Conclusion and outlook	23

1 Introduction

In the pursuit of a fundamental description of particle physics, i.e. of the elementary particles and the interactions between them, theory and experiment necessarily work together towards that goal. Theories are developed based on experimental observations and experiments are designed based on theoretical predictions. Today, the theory that best describes particle physics is the Standard Model of Particle Physics (SM). It is a quantum field theory and as such it describes all fundamental particles as fields and predicts their interactions and the probabilities for the interactions to take place. The SM predictions have been compared to data from particle colliders, from which the same probabilities can be inferred, and excellent agreement has been found. Still, there are phenomena that cannot be explained by the SM, so called Beyond Standard Model (BSM) phenomena, and aspects of the SM that have yet to be tested. Clearly, the need for continued research in this field still exists.

1.1 Detector simulations

At particle colliders, beams of particles are accelerated to a certain energy and then made to collide with each other. In these collisions, the interactions between particles become apparent with formation of new particles from the incoming particles and their energy and the decay of particles into others. What is present after the collision is a myriad of particles, and it is the role of the detectors to record them. It is a task that is made complicated by the difficulties in differentiating between different types of particles, the detector noise, the delay in integrating the signals leading to events piling up, as well as the sheer number of particles present.

When a theory is tested, collisions based on the theory are simulated, and the detector response to the resulting collision products is simulated and compared to the data from the real detector. In this way, an estimate of the likelihood that the theory does indeed describe particle physics can be obtained with a statistical analysis.

The most precise way of simulating the detector response is to simulate the entire geometry of the detector, and the interactions between the particles and the material in each part of it. This is a computationally demanding process though, and faster simulations also exist, at the expense of precision.

1.2 The need for a new detector simulation

In the ATLAS collaboration, both a full simulation of the ATLAS detector and several faster ones exist. Outside such collaborations, though, the benchmark for detector simulations is the generic and parametrized DELPHES [1]. It is fast and gives reasonable results, but for more precise analyses, there is a need for a simulation that is closer to reality, although still fast and freely available. Therefore, a simplified detector simulation has been developed.

1.3 Project outline

The aim of this project was to test the accuracy of the electromagnetic calorimeter of a new detector simulation developed at Uppsala University. The benchmark process chosen for the testing purposes was the decay of the Higgs boson to two photons, $H \rightarrow \gamma\gamma$. This is one of the channels in which the Higgs boson was first observed [2], and so it is well known both theoretically and experimentally. In addition, the decay products interact only with the electromagnetic calorimeter. The process was generated in the event generators MADGRAPH5_AMC@NLO and PYTHIA 8.2 and the generated events were run through the detector simulation with the goal of recreating the well known Higgs peak around $m_H=125$ GeV in the histogram of the invariant mass of the two photons. A big part of the project was to implement a photon reconstruction algorithm needed for calculating the invariant mass. This, and all subsequent analysis was done in the high energy physics data analysis framework ROOT [3]. Background events $pp \rightarrow \gamma\gamma$ were also generated and treated in the same way.

This report is structured as follows: Section 2 gives a short background about detector simulations and presents the software tools used in the analysis, including the Generic detector simulation, as well as the benchmark process. In section 3 the photon reconstruction is described, in section 4 the testing is described in detail and in section 5 the results of the project are presented. The last section is dedicated to conclusions about the project and outlook for further study.

2 Background

2.1 Detector simulations

The simulation of data based on theory proceeds as follows: A list of particles and their four-momenta is generated with *event generators*, i.e. Monte Carlo simulations based on theoretical probabilities, and then run through a *detector simulation*. The goal of a detector simulation is, when treating particles defined in the input, to emulate the response of a real detector hit with the same particles. A generic detector simulation is one that doesn't exactly replicate any existing detector, but is constructed with components common to most detectors. The general structure of particle detectors is described in the next section, followed by a more detailed description of detector simulations and event generators.

2.1.1 Detectors

The ultimate goal of any particle detector is to identify the particles present after a collision and measure their energy and momenta. This is realized in two steps.

First, the detector itself consists of different subdetectors, each designed to supply some information about the incoming particle. These can include

- tracking detectors, in which charged particles make tracks. The tracks can be bent by magnetic fields and used to calculate the momenta of the particles. They can also be matched to measurements in other subdetectors, in which case they supply the charge information of the particles.
- calorimeters, in which particles deposit all their energy through interactions with the material. There are sampling calorimeters and homogenous calorimeters. A sampling calorimeter alternates between *active* material, i.e. material that measures the energy loss of the particles going through it, and *passive* material, i.e. dense material that speeds up the energy loss of the particles, but does not measure anything. A homogenous calorimeter contains only active material. There are electromagnetic calorimeters, mainly supplying information about electrons and photons, and hadronic calorimeters supplying information about hadrons.
- muon systems, which measure muons once they have gone through all the other

subdetectors. This differentiates them from electrons.

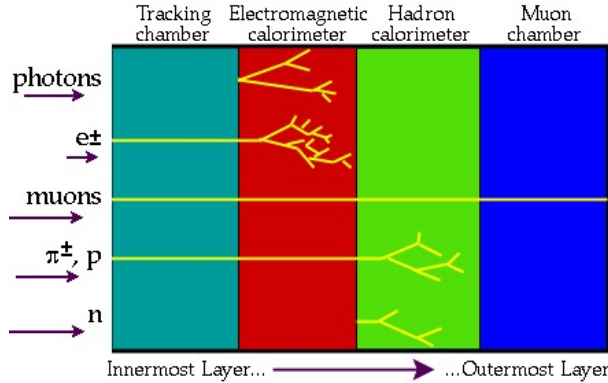


Figure 1: Schematic showing the different subdetectors of a typical particle detector [4]. Some representative particles and their signatures in the detector are shown schematically.

Figure 1 shows schematically how different particles interact with different subdetectors. The subdetectors are built around the beam pipe - the pipe in which the beams collide - with each subdetector built around the previous one. A cross section of this is shown in figure 2.

An example of a particle detector can be seen in figure 3, which shows the subdetectors of the ATLAS detector at the Large Hadron Collider at CERN.

Second, different particle identification (PID) algorithms are used, which combine data from the different subdetectors in order to identify the particles and their energy and momenta.

2.1.2 Simulations

A detector simulation simulates the detector response to incoming particles with different levels of sophistication depending on the simulation. At the fast, but less precise, end of the spectrum are parametrized detector simulations such as DELPHES [1], where no geometry is simulated. On the other end of the spectrum are full simulations of real detectors, such as the full ATLAS simulation, in which the geometry of the ATLAS detector is exactly replicated, and the particle's interactions with the material at its position is simulated in every time step. After the simulation is done, the same PID algorithms as for the data from the real detector are used.

There are a number of ways in which the detector simulations come into play in the process of analyzing high energy particle collisions. The most obvious one

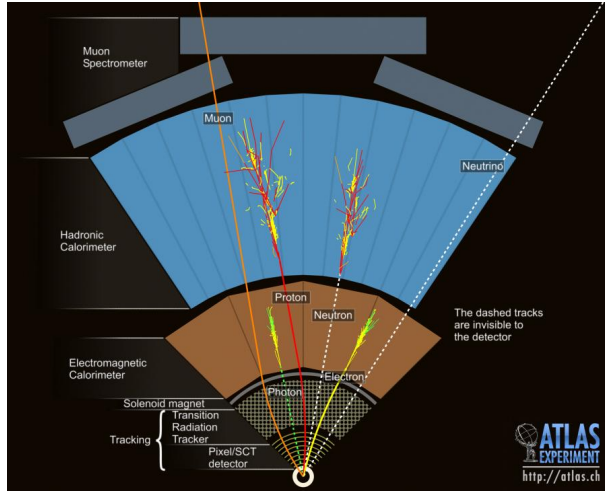


Figure 2: Cross section of a typical configuration of subdetectors around the beam pipe in a particle detector [5]. Some representative particles and their signatures in the detector are shown schematically.

is its direct roll in new physics discoveries, in which a statistical analysis is made to determine the compatibility of the model under study with reality by comparing simulated data to real data. Even before this can be done, however, the detector simulation is used to determine the efficiency of the PID algorithms, and to study how (or even whether) specific predictions can be observed in detector data.

2.1.3 Event generators

Before the detector simulation can be run, the collision has to be simulated. *Event generators* do this by starting from theory and using different methods (e.g. Monte Carlo simulations and/or numerical calculations of cross sections) to generate a list of particles present after the collision together with their energy and momenta. Many different event generators exist, specializing in different aspects of the event, such as different hard processes or the hadronization of gluons and quarks. For the events in this project, two event generators were used: MADGRAPH5_AMC@NLO [7] to generate the hard process, $H \rightarrow \gamma\gamma$, and PYTHIA 8.2 [8] to simulate parton showers and handle hadronization.

MADGRAPH5_AMC@NLO is a matrix element and event generator. It is capable of calculating the matrix elements of any user-defined Lagrangian, and

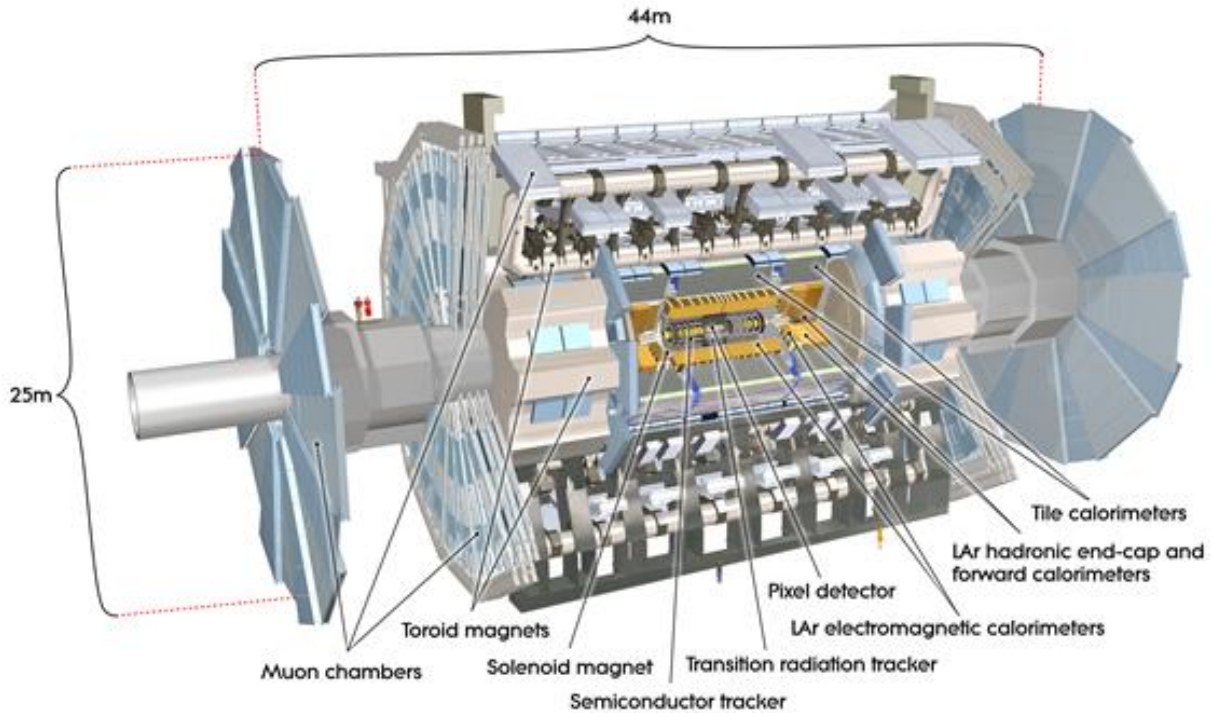


Figure 3: Computer generated image of the whole ATLAS detector [6].

therefore the cross-sections. With the matrix elements as a starting point, it can then generate processes with final states distributed according to the cross-section of the process. There are also a number of models already implemented in MadGraph5_aMC@NLO that can be loaded without having to define a Lagrangian. The default model used is the SM.

PYTHIA 8.2 is a multi-purpose event generator. It can be used on its own, but it can also be interfaced with other matrix element and/or event generators. In the latter case, Pythia takes as an input the processes generated in the third-party program. It then simulates the surrounding partonic activity, such as parton showers, the hadronization of partons and the decay of unstable particles. Here, unstable particles are those that decay before they reach the detector.

2.2 ROOT

ROOT [3] is a framework written in C++ – meaning it is a code package containing libraries of classes – for data analysis in high energy physics. It also contains an interactive interface using the C++ interpreter Cling.

2.2.1 Two important classes

Two of the main features of ROOT are the TTree class, used to store data in a highly compressed format, and the TH1 class used for binning data and visualizing it with histograms.

Trees A TTree is an object designed for storing large quantities of same-class objects. A TTree object is a list of branches (TBranch objects), which in turn is a list of leaves (TLeaf objects). Each leaf contains an object (of the same type as the other leaves), and branches group together leaves that will be read simultaneously. Separate branches can be loaded into memory independently of the other branches in the tree, making working with large files feasible.

Histograms A TH1 object is constructed by giving a name, a range of data and a bin size. It can be filled by feeding it one entry at a time, which is placed in the correct bin. Once it has been filled it can be visualized as a histogram.

2.2.2 Using ROOT

ROOT can be run either in an interactive session by using the Cling prompt or by running compiled C++ code. Commands issued in the Cling prompt can also be collected into a ROOT script, or *macro*, and run through the interpreter.

2.3 Generic Detector Simulation

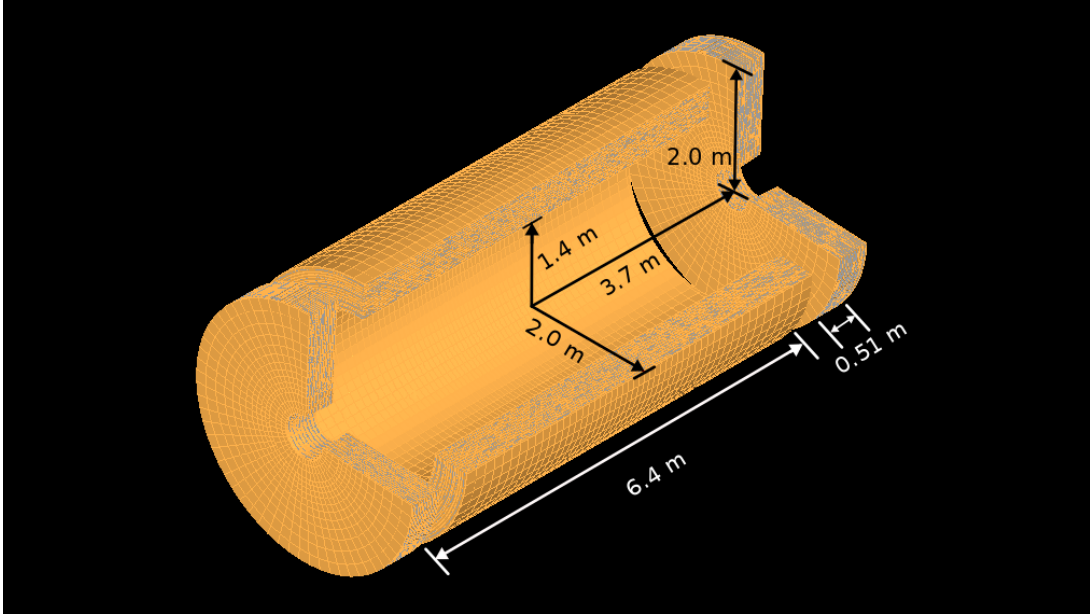
The Generic Detector Simulation is a detector simulation built with the GEANT4 toolkit [9], which simulates the propagation of particles through matter using Monte Carlo methods. It is being developed in the High Energy Physics group at Uppsala University. In the following, only the electromagnetic calorimeter, written by Max Isacson at Uppsala University, will be described.

	Barrel	Outer wheel of endcap	Inner wheel of endcap
$\Delta\eta$	0.05	0.1	0.21
$\Delta\phi$	$\frac{\pi}{32}$	$\frac{\pi}{32}$	$\frac{\pi}{24}$

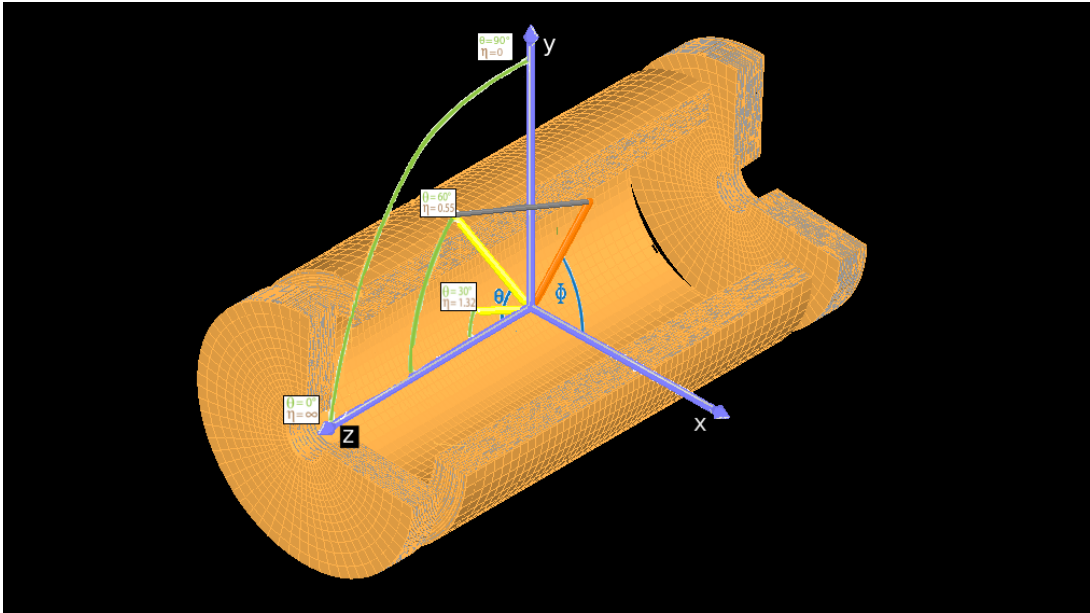
Table 1: The cell sizes in the different sections of the calorimeter

It is a sampling calorimeter and is divided into the barrel region and the endcap region (see 4a). The endcap is further divided into the *inner wheel* (smaller radius) and the *outer wheel* (larger radius). The barrel is 6.4 m long with an inner radius of 1.4 m and an outer radius of 2.0 m. The distance from the center of the barrel to the side of the endcap closest to the center is 3.7 m. The endcap has a depth of 0.51 m and a radius of 2.0 m. The active material in the calorimeter is liquid argon (LAr) and the passive material is lead. At the moment, all energy deposits are recorded directly, also in the passive material.

The calorimeter is segmented into cells, defined in terms of the angles η and ϕ and the distance from the origin r , where ϕ is the azimuthal angle and η is the *pseudorapidity* defined by $\eta = -\ln(\tan(\frac{\theta}{2}))$ where θ is the polar angle. The origin is at the nominal collision point, the z -axis is along the beam pipe, the x - axis points toward the center of the circle and the y -axis points upward. In this coordinate system, $\eta = 0$ is perpendicular to the beam, while $\eta = \pm\infty$ is parallel to it. The coordinate system and some values of η is shown in figure 4b, and table 1 shows the sizes of the cells as well as the boundaries in terms of η of the different sections of the calorimeter.



(a) The measurements of the different parts of the EM calorimeter.



(b) The coordinate system used in the detector and subsequent analysis. Some values of $\eta = -\ln(\tan(\frac{\theta}{2}))$ are shown.

Figure 4: The EM calorimeter of the Generic Detector Simulation. The figure was generated in the Generic Detector Simulation by Max Isacson and then modified by overlaying the measurements and coordinate system.

Incoming particles are propagated through the detector geometry, and the energy

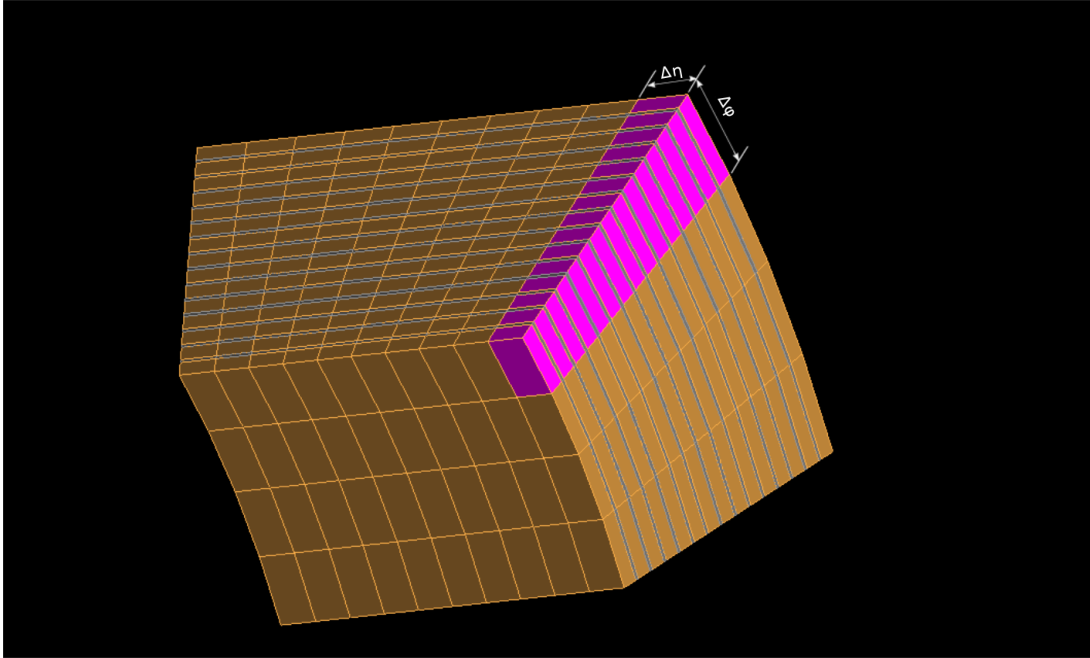


Figure 5: A section of the EM calorimeter barrel. The figure was generated in the Generic Detector Simulation by Max Isacson, and then modified to highlight one tower.

they deposit in each cell is recorded. At the end of the simulation, the energy of all cells with the same η, ϕ coordinates are added radially, creating *towers*.

2.3.1 Using the Generic Detector Simulation

Input into the Generic Detector Simulation is generated by event generators and must be in the HepMC file format. The output is a ROOT-tree in which the presently relevant variables are the (η, ϕ) coordinates of the towers, as well as their energy E .

2.4 Benchmark process $H \rightarrow \gamma\gamma$

The Higgs boson, H , is a scalar particle predicted by the mechanism in the SM that gives mass to massive elementary particles (the Higgs mechanism). It has a narrow theoretical width (4 MeV), so a good energy resolution is needed in the detector in order to make out the peak. The Higgs boson was observed at the LHC in 2012 [10], but Higgs physics is still an active field of research with both the SM and BSM theories containing Higgs bosons being tested at particle accelerators. Due to the importance of the Higgs boson to many theories and the demand that its narrow

width puts on the detector resolution, it serves as a good benchmark for testing a detector simulation. In this project, the decay of the Higgs boson to two photons, $H \rightarrow \gamma\gamma$, has been used for testing purposes. This is because, besides the Higgs boson being a good benchmark, the final state deposits all its energy in the EM calorimeter (see figure 2).

3 Photon Reconstruction

When a photon hits the detector, not all of its energy is deposited in the same tower, but rather in several adjacent ones (see figure 6). To account for all of the energy of the photon, therefore, the energy in these adjacent towers has to be summed up. The idea behind a photon reconstruction algorithm is to find the towers containing energy from the photon and add their energies to form a *cluster*.

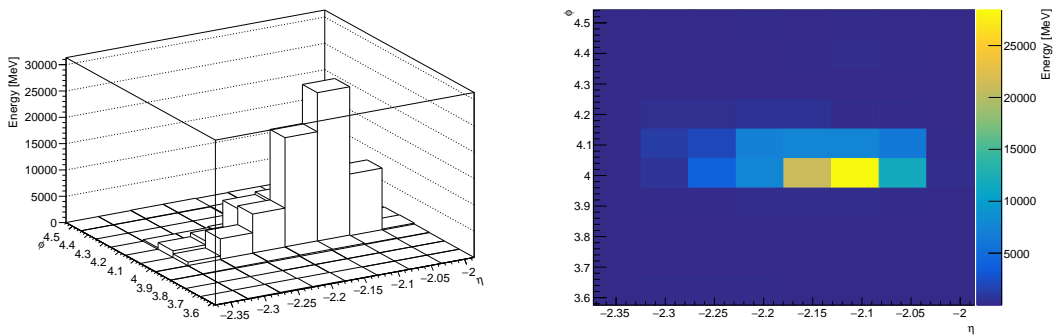


Figure 6: Typical distribution between towers of the energy from one photon hitting the detector in $H \rightarrow \gamma\gamma$ events

A sliding window algorithm was implemented to this end, in which clusters of fixed size are formed. The following description of the algorithm is based on [11], but contains also details specific for the present implementation. The algorithm is run independently for each of the three parts of the detector in which the tower size differs - the barrel, the outer wheel of the endcap and the inner wheel of the endcap.

3.1 Seed positions

The first step of the algorithm is to find the position around which to build the cluster. This is done by letting a $3\Delta\eta \times 3\Delta\phi$ (see table 1) window move across the $\eta\phi$ plane in unit steps of $\Delta\eta$ or $\Delta\phi$. At each point the sum of the transverse energy E_T , i.e. the energy deposited in the transverse direction calculated by $E_T = E \sin(\theta)$, of the 9 towers contained in the window is calculated, as well as its energy weighted barycenter. The sum of the E_T and the position of the barycenter for each point are stored in a two-dimensional array. This array is then iterated through, and when a local maximum in E_T is found, that exceeds a threshold energy of E_T^{thresh} ,

a *precluster* is formed, consisting of the transverse energy and the position of the barycenter of that window. In principle, the sizes of the E_T window and the position window can differ to maximize precluster finding efficiency and minimizing effects of noise, but in this project, the same size has been used for both.

3.2 Removing duplicates

In some cases, more than one local maxima are found inside the same cluster, leading some clusters to be counted more than once. To avoid this, if two preclusters have positions within a window of $2\Delta\eta \times 2\Delta\phi$ of each other, only the precluster with the highest E_T is kept.

3.3 Cluster filling

For each precluster position, the tower containing its position is found. A cluster is then formed with the $3\Delta\eta \times 7\Delta\phi$ towers centered on this tower. Again, the energy weighted barycenter of the cluster is calculated, and this position is used together with the E_T of the cluster to form a four-vector corresponding to the cluster.

4 Analysis

Two datasets were generated: a signal dataset of 2000 $H \rightarrow \gamma\gamma$ events and a background dataset of 5000 $pp \rightarrow \gamma\gamma$ events. The hard processes $H \rightarrow \gamma\gamma$ and $pp \rightarrow \gamma\gamma$ were generated in MADGRAPH5_AMC@NLO with the Higgs effective field theory (heft) and the default SM, respectively. They were then interfaced to PYTHIA8 for parton showers and hadronization.

The datasets were run separately through the detector simulation and the photon reconstruction algorithm described in section 3. A significant simplification was made at this point, since no PID algorithm was used. Instead, it was just assumed that the two clusters with the highest transverse energy were the two photons of the hard process in each event.

5 Results

A histogram of the invariant mass of the two photons in the signal sample is shown in figure 7. A *Crystall Ball function* is fitted to the simulated data. It is given by

$$f(x; \alpha, N, \bar{x}, \sigma) = n \begin{cases} \exp\left(-\frac{(x-\bar{x})^2}{2\sigma^2}\right), & \text{for } \frac{x-\bar{x}}{\sigma} > -\alpha \\ A\left(B - \frac{x-\bar{x}}{\sigma}\right)^{-N}, & \text{for } \frac{x-\bar{x}}{\sigma} \leq -\alpha \end{cases} \quad (1)$$

where

$$\begin{aligned} A &= \left(\frac{N}{|\alpha|}\right)^N \exp\left(-\frac{|\alpha|^2}{2}\right) \\ B &= \frac{N}{|\alpha|} - |\alpha| \\ n &= \frac{1}{\sigma(C+D)} \\ C &= \frac{n}{|\alpha|} \frac{1}{n-1} \exp\left(-\frac{|\alpha|^2}{2}\right) \\ D &= \sqrt{\frac{\pi}{2}} \left(1 + \operatorname{erf}\left(\frac{|\alpha|}{\sqrt{2}}\right)\right) \end{aligned}$$

Here α , N , \bar{x} and σ are parameters to be fitted to the data. The crystal ball function has the form of a Gaussian with a power-law tail extending down below a certain threshold related to α . \bar{x} is the mean of the Gaussian and σ its standard deviation. N is the inverse power of the power-law tail, and n is a normalization constant. erf is the error function given by

$$\operatorname{erf}(x) = \frac{2}{\sqrt{\pi}} \int_0^x e^{-t^2} dt \quad (2)$$

The mean value of the invariant mass in the signal sample is 120.9 GeV with a standard deviation of 1.868 GeV. These results can be compared with the observed mass of the Higgs boson, $m_H = 125.18 \pm 0.16$ GeV [12], and to the results from the first observation of the Higgs boson [2], shown in figure 8.

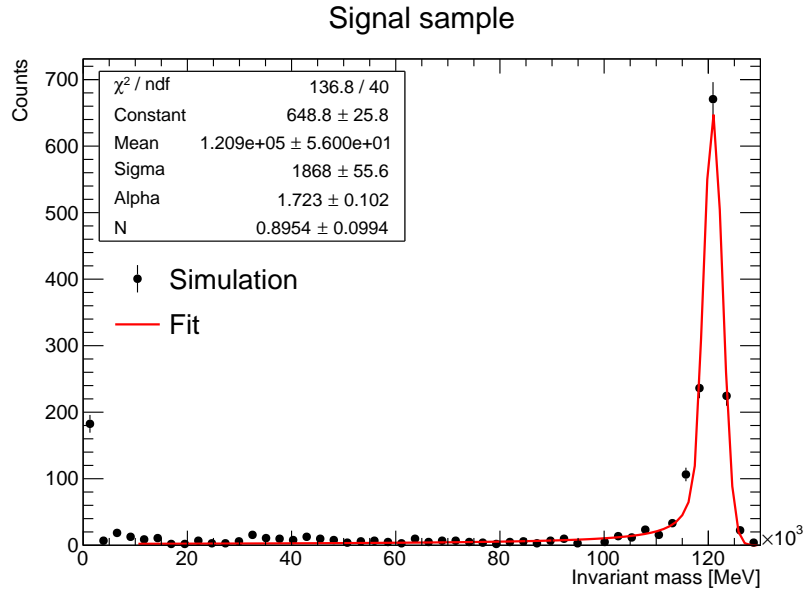


Figure 7: The invariant mass of the two photons in the signal sample. Scaled so that the integral is the expected number of $H \rightarrow \gamma\gamma$ at $\mathcal{L} = 36000 \text{ pb}^{-1}$. Fitted with a Crystal Ball function. The peak at invariant mass 0 GeV is most likely due to converted photons, as discussed in the text. The parameters Constant and Mean from the figure correspond to n and \bar{x} of equation 1, respectively.

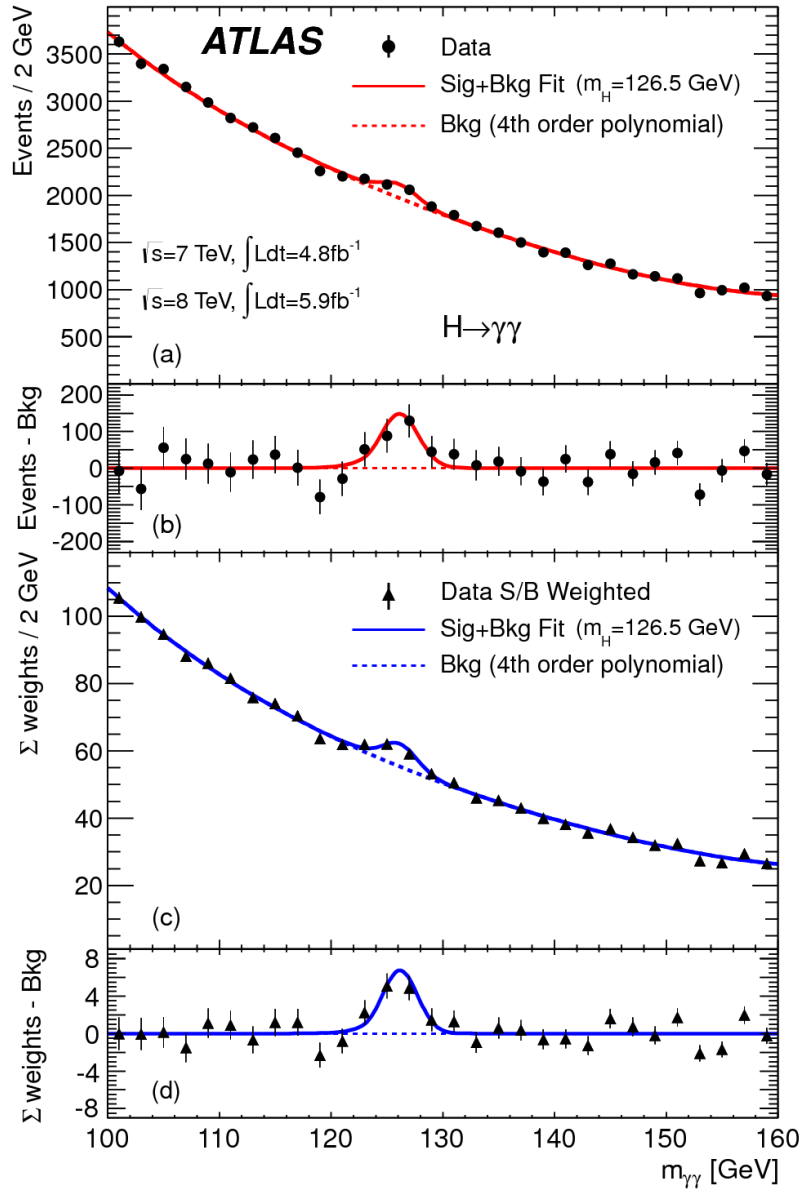


Figure 8: Published in Phys.Lett. B716 (2012) 1-29. The distributions of the invariant mass of diphoton candidates after all selections for the combined 7 TeV and 8 TeV data sample. The inclusive sample is shown in a) and a weighted version of the same sample in c); the weights are explained in the publication. The result of a fit to the data of the sum of a signal component fixed to $m_H = 126.5$ GeV and a background component described by a fourth-order Bernstein polynomial is superimposed. The residuals of the data and weighted data with respect to the respective fitted background component are displayed in b) and d).

The mean value in the simulated data is slightly lower than m_H , but the standard deviation of the sample is comparable to the experimental one - it is close to 2 GeV in both cases.

The peak at 0 GeV seen in the signal spectrum is most likely due to converted photons, i.e. an electron/positron pair originating from a single high-energy photon, since the algorithm doesn't differentiate between photons and electrons/positrons. This is further supported by the plot shown in fig 9, in which the distance $\Delta R = \sqrt{\Delta\eta^2 + \Delta\phi^2}$ between the two clusters with the highest E_T is plotted against their invariant mass. This shows that when the invariant mass is close to 0 GeV, the distance between the clusters is close to 0, which is consistent with the idea that the two clusters actually correspond to an electron/positron pair originating from one high energy photon.

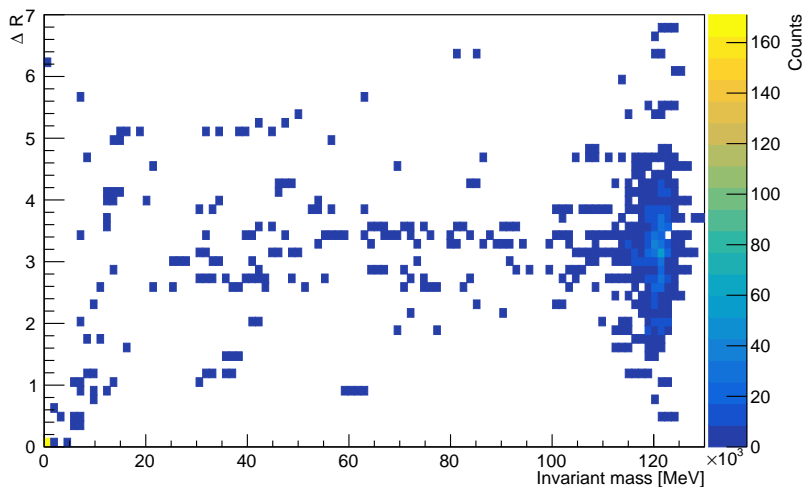


Figure 9: The distance $\Delta R = \sqrt{\Delta\eta^2 + \Delta\phi^2}$ plotted against the invariant mass of the two clusters with the highest E_T . The distance between the clusters is close to 0 when the invariant mass is close to 0 GeV, supporting the idea that these clusters are in fact a converted photon.

Figure 10 shows the invariant mass of the two photons in the background sample.

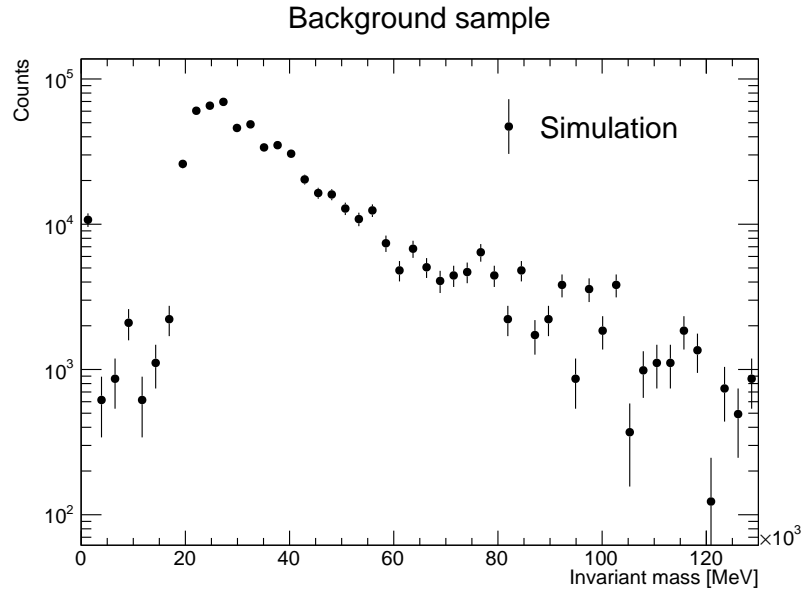


Figure 10: The invariant mass of the two photons in the background sample. Scaled so that the integral is the expected number of $pp \rightarrow \gamma\gamma$ at $\mathcal{L} = 36000 \text{ pb}^{-1}$.

Figure 11 shows the spectrum obtained by adding the signal and background samples (while both normalized to their respective expected number of events at $\mathcal{L} = 36000 \text{ pb}^{-1}$). The Higgs peak cannot be distinguished from the statistical fluctuations. This can be remedied with a bigger dataset.

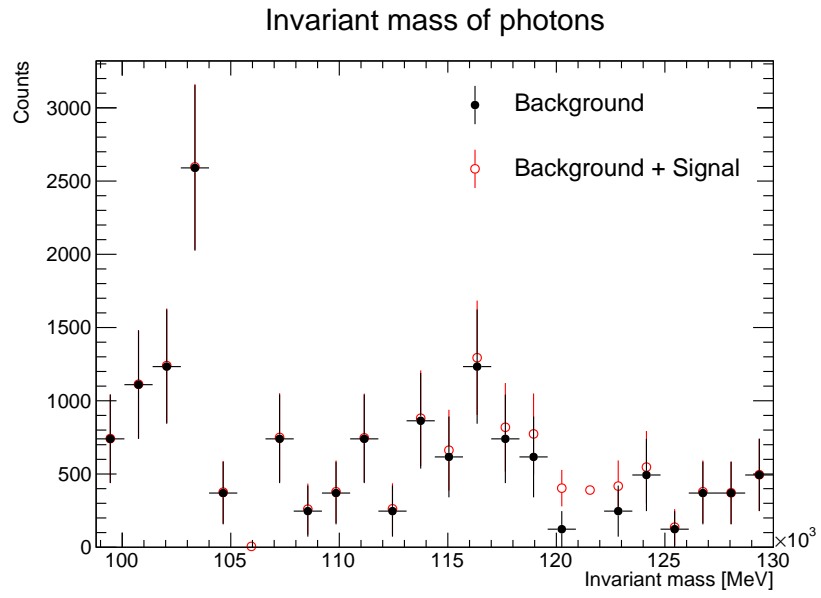


Figure 11: The invariant mass of the two photons in the added background and signal sample. Scaled so that the integral is the expected number of $pp \rightarrow \gamma\gamma$ and $H \rightarrow \gamma\gamma$ events at $\mathcal{L} = 36000 \text{ pb}^{-1}$.

6 Conclusion and outlook

This project has demonstrated that the Generic Detector Simulation can recreate the Higgs peak from generated $H \rightarrow \gamma\gamma$ events, with a width consistent with experimental data and a mean that is slightly below the Higgs mass $m_H = 125$ GeV. The discrepancy between the generated mass and the simulation output can most likely be rectified by calibration of the clusters used in the photon reconstruction. No estimate of the accuracy of the detector simulation when it comes to signal-to-background ratios could be made since the datasets were too small to draw statistically significant conclusions from. A natural immediate next step is therefore to generate more data and to calibrate the clusters. Beyond that are many possibilities for further study, such as using the tracking detector together with the calorimeter and implementing PID algorithms, as well as simulating pile-up.

References

- [1] The DELPHES 3 collaboration, J. de Favereau, C. Delaere, P. Demin, A. Giammanco, V. Lemaître, A. Mertens, and M. Selvaggi. Delphes 3: a modular framework for fast simulation of a generic collider experiment. *Journal of High Energy Physics*, 2014(2):57, Feb 2014.
- [2] ATLAS Collaboration. Observation of a new particle in the search for the Standard Model Higgs boson with the ATLAS detector at the LHC. *Phys. Lett.*, B716:1–29, 2012.
- [3] R. Brun and F. Rademakers. ROOT: An object oriented data analysis framework. *Nucl. Instrum. Meth.*, A389:81–86, 1997.
- [4] http://www.particleadventure.org/images/page-elements/decay_chart.gif. Accessed: 2018-09-12.
- [5] Joao Pequena. Event Cross Section in a computer generated image of the ATLAS detector. CERN-GE-0803022, <https://cds.cern.ch/record/1096081>, Mar 2008.
- [6] Joao Pequena. Computer generated image of the whole ATLAS detector. CERN-GE-0803012, <https://cds.cern.ch/record/1095924>, Mar 2008.
- [7] J. Alwall, R. Frederix, S. Frixione, V. Hirschi, F. Maltoni, O. Mattelaer, H. S. Shao, T. Stelzer, P. Torrielli, and M. Zaro. The automated computation of tree-level and next-to-leading order differential cross sections, and their matching to parton shower simulations. *JHEP*, 07:079, 2014.
- [8] Torbjörn Sjöstrand, Stefan Ask, Jesper R. Christiansen, Richard Corke, Nishita Desai, Philip Ilten, Stephen Mrenna, Stefan Prestel, Christine O. Rasmussen, and Peter Z. Skands. An Introduction to PYTHIA 8.2. *Comput. Phys. Commun.*, 191:159–177, 2015.
- [9] S. Agostinelli et. al. Geant4—a simulation toolkit. *Nuclear Instruments and Methods in Physics Research Section A: Accelerators, Spectrometers, Detectors and Associated Equipment*, 506(3):250 – 303, 2003.
- [10] ATLAS Collaboration. The ATLAS Experiment at the CERN Large Hadron Collider. *JINST*, 3:S08003, 2008.

- [11] W. Lampl, S. Laplace, D. Lelas, P. Loch, H. Ma, S. Menke, S. Rajagopalan, D. Rousseau, S. Snyder, and G. Unal. Calorimeter clustering algorithms: Description and performance. 2008. ATL-LARG-PUB-2008-002, ATL-COM-LARG-2008-003.
- [12] Particle Data Group. Review of particle physics. *Phys. Rev. D*, 98:030001, Aug 2018.